Real-Time stack monitoring at the BaTek medical isotope production facility

Article *in* Journal of Radioanalytical and Nuclear Chemistry · July 2015

DOI: 10.1007/s10967-015-4348-2

Real-time stack monitoring at the BaTek medical isotope production facility

Justin I. McIntyre, Agung Agusbudiman, Ian M. Cameron, Johannes R. Dumais, Paul W. Eslinger, Abdelhakim Gheddou, Kirill Khrustalev, et al.

Journal of Radioanalytical and Nuclear Chemistry
An International Journal Dealing with All Aspects and Applications of Nuclear Chemistry

ISSN 0236-5731

J Radioanal Nucl Chem
DOI 10.1007/s10967-015-4348-2

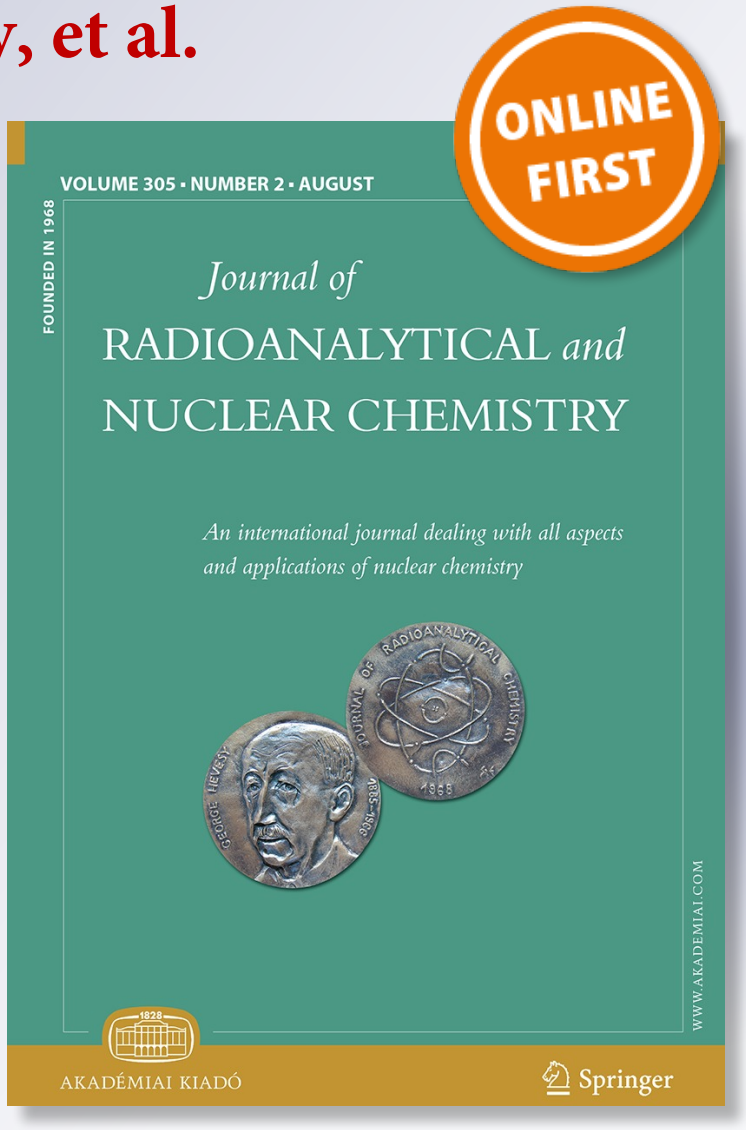

Springer

J Radioanal Nucl Chem
DOI 10.1007/s10967-015-4348-2

Real-time stack monitoring at the BaTek medical isotope production facility

Justin I. McIntyre[1] · Agung Agusbudiman[2] · Ian M. Cameron[1] · Johannes R. Dumais[2] · Paul W. Eslinger[1] · Abdelhakim Gheddou[3] · Kirill Khrustalev[3] · Pujadi Marsoem[2] · Harry S. Miley[1] · Mika Nikkinen[4] · Amanda M. Prinke[1] · Michael D. Ripplinger[1] · Brian T. Schrom[1] · William A. Sliger[1] · Ulrich Stoehlker[5] · Gatot Suhariyono[2] · Glen A. Warren[1] · Susilo Widodo[2] · Vincent T. Woods[1]

Received: 10 July 2015

Abstract Radioxenon emissions from fission-based radiopharmaceutical production are a major source of background concentrations affecting the radioxenon detection systems of the international monitoring system (IMS). Collection of real-time emissions data from production facilities makes it possible to screen out some medical isotope signatures from the IMS radioxenon data sets. This paper describes an effort to obtain and analyze real-time stack emissions data with the design, construction and installation of a small stack monitoring system developed by a joint CTBTO-IDC, BATAN, and Pacific Northwest National Laboratory team at the BaTek medical isotope production facility near Jakarta, Indonesia.

Keywords Medical isotope production · International monitoring system (IMS) · Stack monitoring · Radioxenon · CTBTO

Introduction

The production of fission-based radiopharmaceuticals is a major source of anthropogenic radioxenon in the atmosphere. Production of ^{99}Mo, the precursor for ^{99m}Tc, is of particular interest, because it is typically generated by irradiating a uranium target. Molybdenum-99 comprises about 6 % of the fission atoms produced in this process, and the global demand for ^{99}Mo is on the order of 10,000 6-day curies (Ci) per week [1], enough for approximately 20 million patient doses per year. The two noble gas isotopes ^{133}Xe and ^{135}Xe are also produced in similar quantities [2] and they are released to the air when the uranium is chemically dissolved. Without a trapping scheme, practically all of the xenon produced during radiopharmaceutical creation will be released to the atmosphere.

These emissions affect the radioxenon detection systems of the international monitoring system (IMS) [3], causing several thousand detections a year at the radioxenon stations [4, 5]. Some of these emissions are large enough to have the potential to mask small radioxenon emissions from underground nuclear explosions [6, 7].

With careful atmospheric modeling (ATM) it is possible to distinguish between radioxenon releases from nuclear explosions and civilian activities [8] if several isotopes are measured simultaneously within the same air sample. This is possible because emissions from nuclear power plants and medical isotope production facilities have different isotopic mixes.

Medical isotope production facilities use different irradiation profiles and separations processes, thus it is useful to develop facility-specific radioxenon isotopic signatures. When real-time release data are available, it may be possible to use ATM and isotopic ratios to screen out radiopharmaceutical medical isotope radioxenon signatures from the daily world-wide IMS radioxenon data sets [4]. Past efforts working with several medical isotope production facilities have proven very successful in terms of stack monitoring, and in one case an efficient xenon retention system has abated stack emissions to less than 5×10^9 Bq

✉ Paul W. Eslinger
paul.w.eslinger@pnnl.gov

[1] Pacific Northwest National Laboratory, Richland, WA, USA

[2] BATAN, National Nuclear Energy Agency, Jakarta, Indonesia

[3] International Data Centre, CTBTO, Vienna, Austria

[4] International Atomic Energy Agency, Vienna, Austria

[5] Federal Office for Radiation Protection, Freiburg, Germany

Published online: 30 July 2015

per day [9], a level that has been determined to have little impact on IMS detection systems [10].

In 2012, a joint CTBTO-BATAN-PNNL team developed and deployed a simple stack monitor at the PT. BATAN Teknologi (BaTek) medical isotope production facility near Jakarta, Indonesia. The stack monitor was designed to provide near-real time gamma-ray spectroscopic data so four radioxenon isotopes (^{131m}Xe, ^{133m}Xe, ^{133}Xe, and ^{135}Xe) could be identified and quantified throughout the uranium dissolution process cycle at the facility.

Experimental

The project team set a goal of developing a low-cost stack-air monitoring system that integrated with existing facility infrastructure and equipment with a minimum of impact on operations while providing high-quality data. The following five general design requirements were identified: (1) Provide a known volume and geometry for stack gases to occupy during counting, (2) design the sample holder to mate with a $LaBr_3$(Cl) detector, (3) measure the air flow through the system and provide active airflow assistance to facilitate rapid sample turnover, (4) use a modest amount of lead shielding to reduce the non-sample-related radiometric background, and (5) incorporate a charcoal filter unit upstream of the sampling volume to reduce potential contamination by other isotopes.

A schematic of the sampling system is provided in Fig. 1. The overall cost in parts was less than $26,000 (U.S.) and included $11,000 for the $LaBr_3$(Cl) detector, manufactured by Saint-Gobain, with multichannel spectroscopic readout and a laptop PC [11]. The sample volume was a 1-l gas-tight Marinelli GA-MA G-133N beaker surrounded by 2.5 cm of lead. The air flow and temperature were continuously measured by a Red-y^{TM} unit (manufactured by Vögtlin Instruments AG-flow technology) that interfaced with the PC via a USB connector. The detector housing was a model DC2011 manufactured by Canberra Packard. A compressor pump was used to exchange air volumes in the 1-l sample volume. A charcoal filter was placed upstream to significantly reduce the amount of radioiodine in the airflow because radioiodine will plate out on the Marinelli beaker and interfere with some of the radioxenon decay peaks.

A scintillator detector was selected over other detector designs due to expected high count rates, a long deployment time and the lack of daily technician support. The $LaBr_3$(Cl) detector was the highest resolution commercially available scintillator at the time of purchase.

The BaTek facility had commercial radiation health and safety monitoring equipment integrated into the airflow of the stack; the new sampling and detection system was installed in the existing airflow system with minimal changes to the existing piping.

Detector and counting cell geometry calculations

The $LaBr_3$(Ce) detector was modeled using GEANT4, version 9.5 patch 1 [12] to estimate its detection efficiency for various decay energies. The detector geometry consists of the 3.8 cm diameter by 3.8 cm long $LaBr_3$(Ce) crystal, a photomultiplier tube and base, a detector container, the sample beaker and lead shielding. The photomultiplier tube is a simple aluminum cylinder, although for modeling purposes the density of the aluminum was chosen to have the same mass as an annulus with the same outer diameter

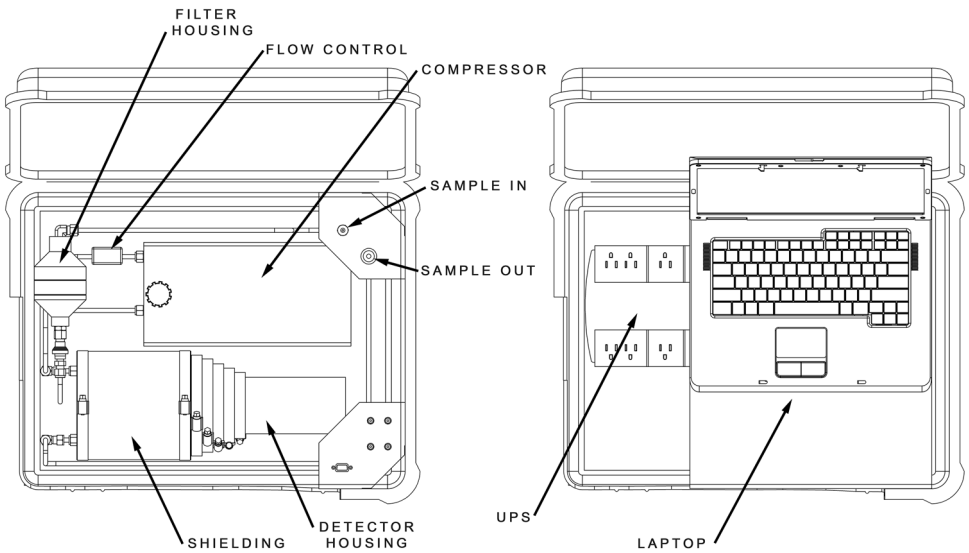

Fig. 1 Schematic of the gamma-ray detector/air sampling system

and 1-mm thick walls. The modeled detector enclosure was a simplified geometry of the Canberra DC2011 scintillator enclosure. No holes for gas tubes were included in the model.

Four noble gas sources and four check sources were simulated. The energy deposition in the LaBr crystal was recorded during the simulations; the optical photons were not modeled. The noble gas sources (^{133}Xe, ^{135}Xe, ^{85}Kr and ^{88m}Kr) were distributed uniformly within the sample beaker, whereas the check sources used for benchmarking measurements (^{60}Co, ^{133}Ba, ^{137}Cs and ^{241}Am) were placed in the center of the top of the beaker. The lead shielding was removed from the model while modeling the benchmarking measurements. Energy resolution was not incorporated into the modeled response because the comparisons focused on the strengths of selected peaks.

Benchmarking measurements

A series of measurements with check sources was conducted after the system was delivered to the BaTek facility. The sources consisted of ^{60}Co, ^{133}Ba, ^{137}Cs and ^{241}Am. Each measurement was conducted over a 600-s time interval. A comparison of the peak strengths from the GEANT4 simulations and the measurements is shown in Table 1. The quantity recorded in the table is the number of counts per one thousand decays. For the measurement spectra, the strengths of the peaks were determined using fits to the data assuming a quadratic background. The average result over the available runs for each isotope is reported in Table 1 along with one standard deviation error bars.

The simulated and measured results for the 384-keV peak of ^{133}Ba are different enough that the 384-keV result was excluded from the analysis. The relative strength of the 384- to 356-keV peaks is 0.144 [13], while in the simulation it is 0.196 (assuming essentially no difference in detector efficiency for the two energy levels). This difference suggests that the simulated strength of the 384-keV peak is too strong.

The energies of the calibrations are clustered together by source type, with little overlap between sources. This clustering makes it difficult to ascertain whether the apparent energy dependence of the ratio is due to an incorrect energy dependence of the simulation, experimental issues related to the use of the sources, or a source-dependent normalization problem. For purposes of this analysis, a simple average of the ratios of the simulated strengths to the measured strengths was 1.04 with a standard deviation of 0.15.

Energy calibration

Several additional GEANT4 simulations were conducted to estimate the efficiency of the detector to photons at various energies. The simulations randomly generated the initial position of the photons inside the beaker and assumed an isotopic angular distribution. The calibrations were conducted with version 9.5 patch 2 of GEANT4, using the physics libraries distributed with that version. This is a change from previous simulations, which used version 9.5 patch 1. No significant differences for simulated ^{133}Xe results were observed between the two different versions. Detector efficiencies for a range of energies are provided in Table 2.

Results and discussion

Gamma spectra were collected and digitally stored from February 1, 2013, to December 22, 2013. The detector collected data approximately 80 % of the time the facility

Table 1 Comparison of simulated and measured peak strengths

Energy (keV)	Source	Measurement (Cts/k-decay)	Simulation (Cts/k-decay)	Ratio of simulated to measured
59	^{241}Am	3.32 ± 0.10	3.151 ± 0.010	0.949 ± 0.029
81	^{133}Ba	2.782 ± 0. 087	2.213 ± 0.008	0.796 ± 0.025
276	^{133}Ba	0.345 ± 0.011	0.335 ± 0.003	0.971 ± 0.031
303	^{133}Ba	0.824 ± 0.025	0.923 ± 0.005	1.120 ± 0.034
356	^{133}Ba	2.432 ± 0.073	2.727 ± 0.009	1.121 ± 0.034
384	^{133}Ba	0.316 ± 0.010	0.535 ± 0.004	1.694 ± 0.056
662	^{137}Cs	1.774 ± 0.063	2.297 ± 0.008	1.295 ± 0.046
1172	^{60}Co	1.165 ± 0.036	1.231 ± 0.006	1.057 ± 0.033
1332	^{60}Co	1.034 ± 0.032	1.076 ± 0.006	1.041 ± 0.033

Table 2 Detection efficiency for different gamma energies

Energy (keV)	Efficiency (%)
50	2.39
75	2.72
100	2.79
125	2.77
150	2.65
200	2.41
250	2.05
300	1.75
400	1.31
500	1.03
750	0.661
1000	0.495
1500	0.335
2000	0.249
2500	0.188
3000	0.153

was operating. The stored data sets were analyzed at Pacific Northwest National Laboratory (PNNL). Xenon radionuclides analyzed for this publication are listed in Table 3 along with the relevant physical and detector characteristics.

The measurement campaign collected approximately 25,000 individual gamma-ray spectra at 10-min intervals. Individual spectra were integrated to provide a collection period of 1 h and releases were then calculated for specific isotopes with known emission energies. The estimated amount of each isotope was based on a separate energy peak. The emission profile under inspection was fit to specific peaks using a polynomial background description and a Gaussian curve component using the following equation:

$$F_{\mathrm{p}}(x) = c_0 + c_1 x + c_2 x^2 + A_{\mathrm{p}} e^{-\frac{(x-\mu_{\mathrm{p}})^2}{2\sigma_{\mathrm{p}}^2}}. \quad (1)$$

The background is estimated by fitting a quadratic equation to adjoining samples on both sides of the peak while omitting data in the peak. The background values are subtracted before the Gaussian (exponential) term in Eq. (1) is fit to the data. The mean value of the specific peak, μ_{p}, and the spread parameter, σ_{p}, are estimated from the background-adjusted data along with the coefficient A_{p}. If the mean of the Gaussian term in Eq. (1) was more than 5 keV away from the theoretical peak or the spread was more than 15 keV, then the data spectrum was discarded as not containing the isotope of interest.

A typical gamma spectrum is shown in the left pane of Fig. 2. The right pane of Fig. 2 illustrates the region of interest for ^{135}Xe, with the data, polynomial background fit and resulting Gaussian fit.

The spectra were analyzed for the noble gas radioisotopes ^{133}Xe and ^{135}Xe. These radioisotopes were typically observed in the range of 10^3–10^7 counts per hour, as illustrated in Fig. 3.

Release estimates (Bq) were calculated for each hour using the formula

$$R_{\mathrm{p}} = \frac{C_{\mathrm{p}}}{B_{\mathrm{ratio}} \cdot D_{\mathrm{eff}}} \cdot \mathrm{Flow}_{\mathrm{stack}} \cdot \Delta t \quad (2)$$

The coefficient C_{p} is the number of counts in the peak obtained from summing the Gaussian fit from Eq. (1) at the set of discrete energy levels near the peak, B_{ratio} is the branching ratio for the isotope for the specific energy peak, D_{eff} is the detector efficiency at the specific peak energy, $\mathrm{Flow}_{\mathrm{stack}}$ is air flow rate through the stack ($\mathrm{m}^3\ \mathrm{h}^{-1}$) and Δt is the sample collection time (h). The facility air flow rate is a constant $2.2 \times 10^4\ \mathrm{m}^3\ \mathrm{h}^{-1}$.

As a validation exercise, the amount of ^{133}Xe produced during the irradiation process is calculated from the amount of ^{99}Mo produced and compared to the release estimates. The medical isotope production facility has the capacity to produce about 100 6-day Ci of ^{99}Mo ($T_{1/2} = 2.75$ days) per week although the historical production averages near 40 6-day Ci of ^{99}Mo per week. If there are 100 Ci (3.7×10^{12} Bq) of ^{99}Mo remaining 6 days after being packaged for distribution, then about 1.68×10^{13} Bq of ^{99}Mo was present at the time of packaging. If packaging occurs approximately 1 week after discharge from the reactor, then about 9.82×10^{13} Bq of ^{99}Mo was present at the time of discharge from the reactor. We assume that the activity of ^{133}Xe is equal to the activity of ^{99}Mo at the time of discharge from the reactor [2]. Although the duration of cooling periods and the timing of chemical dissolution and air venting actions vary from batch to batch, we make the assumption that the majority of the resulting ^{133}Xe is vented through the stack halfway between discharge from the reactor and the time of packaging. Using this crude timing assumption, about 6×10^{11} Bq of ^{133}Xe may be vented for every 6-day Ci of ^{99}Mo produced.

The stack data for June 15–21, 2013 show a release of 1.84×10^{13} Bq of ^{133}Xe. Concentrations of ^{133}Xe in the

Table 3 Xenon isotopes identified from gamma spectra

Isotope	Peak energy (keV)	Half-life	Branching ratio (%)	Detector efficiency (%)
^{135}Xe	249.8	9.14 h	90.0	2.05
^{133}Xe	81.0	5.25 days	36.9	2.75

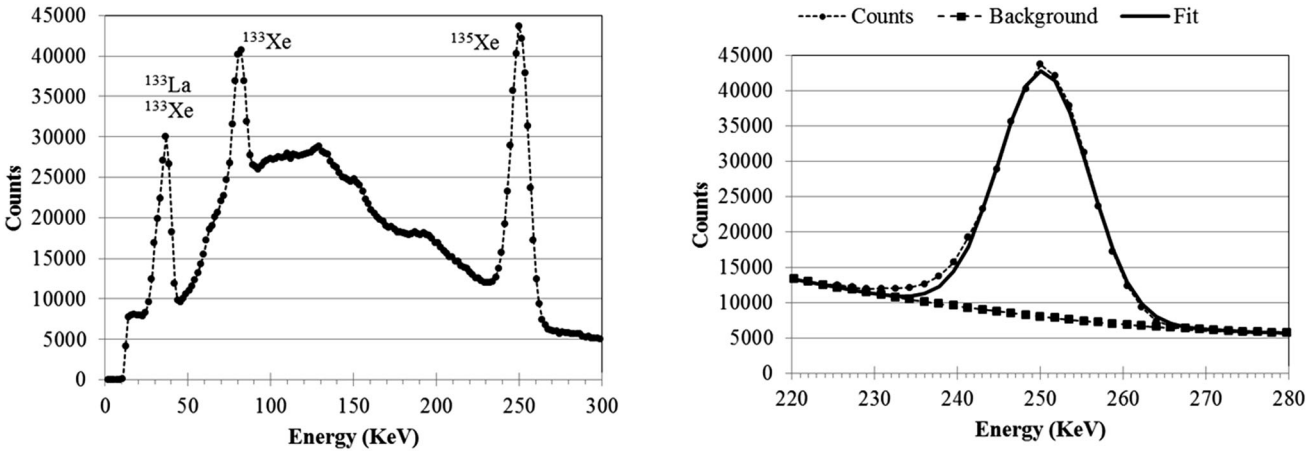

Fig. 2 *Left pane* Typical gamma spectra. *Right pane* Example of the fitting algorithm results for the ^{135}Xe peak fit

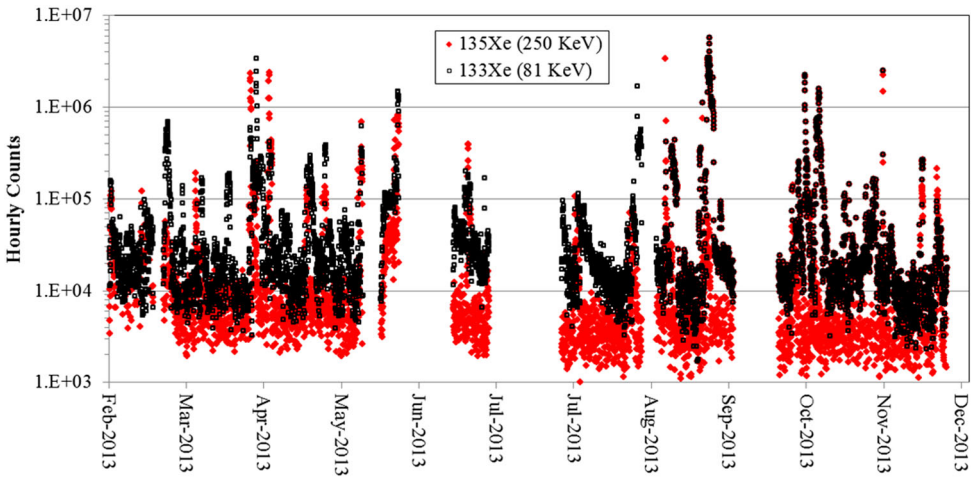

Fig. 3 Hourly count data for ^{133}Xe and ^{135}Xe

air are available at the same time from a xenon sampler located 14 km from BaTek. An optimization process [14] using atmospheric transport modeling and the sampler air concentrations produced a release estimate of 1.88×10^{13} Bq. The same optimization process yielded a release estimate of 1.70×10^{13} Bq for a different week in 2012. The stack release value and the two optimized estimates are all within 10 % of each other.

Except for one 3-day period, the stack sampler collected data for the entire months of February, March and April of 2013. The facility produced 590 6-day Ci of ^{99}Mo over this three-month period. The calculated stack releases over these 3 months results in an estimated release of 4.3×10^{11} Bq of ^{133}Xe per 6-day Ci of ^{99}Mo. This is 72 % of the approximate release value derived from fission and rough decay time arguments, and indicates good agreement, especially when 1 day of delay in the release of ^{133}Xe reduces the released quantity by over 12 %. The stack sampler measured an average daily release of 2.8×10^{12} Bq of ^{133}Xe for February, March and April of 2013. The average daily release of ^{135}Xe was 6.5×10^{12} Bq for the same time period.

Although a detailed system-level uncertainty analysis was not performed for these calculations, there is about a 15 % uncertainty associated with the calculations prior to using Eq. (2) to convert counts in the sampler to activity released from the stack. The dominant, but unknown, uncertainty in Eq. (2), and the dominant uncertainty in estimates of releases to the environment, is the flow rate of air through the stack. The good agreement between the calculated releases and estimates of possible releases based on the fission yield indicates that the nominal air flow rate assumed for this work is reasonable.

Conclusions

A small stack monitoring system developed by a joint CTBTO-IDC, BATAN, and PNNL team was deployed at the BaTek medical isotope production facility near Jakarta,

Indonesia. The low-cost stand-alone monitoring system proved reliable in operation and minimal facility changes were required for installation in an existing exhaust air system. The detector system used commercially available components and a portable computer. This type of system could easily be deployed in other facilities without an active monitoring system.

The average daily release from the BaTek medical isotope production facility for February, March and April of 2013 was 2.8×10^{12} Bq of ^{133}Xe and 6.5×10^{12} Bq of ^{135}Xe. These releases are reasonable given the production of 590 6-day Ci of ^{99}Mo during this time period and a facility design that does not significantly delay the release of exhaust air to allow decay to reduce activity of the released isotopes.

Acknowledgments The authors wish to acknowledge the funding support of the U.S. Office of Multilateral and Nuclear Affairs in the Bureau of Arms Control, Verification and Compliance Nuclear, at the Department of State and the U.S. Nuclear Arms Control Technology Program, at the Defense Threat Reduction Agency. The stack monitor equipment and data analysis to support the CTBTO in implementing the noble gas verification regime were funded by the European Union through Council Joint Action 2008/588/CFSP of 15 July 2008.

References

1. OECD (2014) Medical Isotope Supply in the Future: Production Capacity and Demand Forecast for the ^{99}Mo/^{99m}Tc Market, 2015–2020. vol NEA/SEN/HLGMR(2014)2. Nuclear Energy Agency. Organisation for Economic Co-Operation and Development, Paris, France
2. Chadwick MB, Herman M, Obložinský P, Dunn ME, Danon Y, Kahler AC, Smith DL, Pritychenko B, Arbanas G, Arcilla R, Brewer R, Brown DA, Capote R, Carlson AD, Cho YS, Derrien H, Guber K, Hale GM, Hoblit S, Holloway S, Johnson TD, Kawano T, Kiedrowski BC, Kim H, Kunieda S, Larson NM, Leal L, Lestone JP, Little RC, McCutchan EA, MacFarlane RE, MacInnes M, Mattoon CM, McKnight RD, Mughabghab SF, Nobre GPA, Palmiotti G, Palumbo A, Pigni MT, Pronyaev VG, Sayer RO, Sonzogni AA, Summers NC, Talou P, Thompson IJ, Trkov A, Vogt RL, van der Marck SC, Wallner A, White MC, Wiarda D, Young PG (2011) ENDF/B-VII.1 Nuclear Data for Science and Technology: cross sections, covariances, fission product yields and decay data. Nucl Data Sheets 112(12):2887–2996. doi:10.1016/j.nds.2011.11.002
3. CTBTO (2013) Comprehensive nuclear-test-ban-treaty organization (CTBTO) preparatory Commission Web Page. http://www.ctbto.org/. Accessed 19 Sept 2013
4. Saey PRJ, Ringbom A, Bowyer TW, Zähringer M, Auer M, Faanhof A, Labuschagne C, Al-Rashidi MS, Tippawan U, Verboomen B (2012) Worldwide measurements of radioxenon background near isotope production facilities, a nuclear power plant and at remote sites: the ''EU/JA-II'' Project. J Radioanal Nucl Chem. doi:10.1007/s10967-012-2025-2
5. Wotawa G, Becker A, Kalinowski M, Saey P, Tuma M, Zähringer M (2010) Computation and analysis of the global distribution of the radioxenon isotope ^{133}Xe based on emissions from nuclear power plants and radioisotope production facilities and its relevance for the verification of the nuclear-test-ban treaty. Pure Appl Geophys 167(4–5):541–557. doi:10.1007/s00024-009-0033-0
6. Ringbom A, Axelsson A, Aldener M, Auer M, Bowyer TW, Fritioff T, Hoffman I, Khrustalev K, Nikkinen M, Popov V, Popov Y, Ungar K (2013) Wotawa G (2014) Radioxenon detections in the CTBT international monitoring system likely related to the announced nuclear test in North Korea on February 12. J Environ Radioact 128:47–63. doi:10.1016/j.jenvrad.2013.10.027
7. Becker A, Wotawa G, Ringbom A, Saey PRJ (2010) Backtracking of noble gas measurements taken in the aftermath of the announced October 2006 event in North Korea by means of PTS methods in nuclear source estimation and reconstruction. Pure Appl Geophys 167(4):581–599. doi:10.1007/s00024-009-0025-0
8. Kalinowski M, Axelsson A, Bean M, Blanchard X, Bowyer T, Brachet G, Hebel S, McIntyre J, Peters J, Pistner C, Raith M, Ringbom A, Saey P, Schlosser C, Stocki T, Taffary T, Kurt Ungar R (2010) Discrimination of nuclear explosions against civilian sources based on atmospheric xenon isotopic activity ratios. Pure Appl Geophys 167(4):517–539. doi:10.1007/s00024-009-0032-1
9. Zähringer M, Becker A, Nikkinen M, Saey P, Wotawa G (2009) CTBT radioxenon monitoring for verification: today's challenges. J Radioanal Nucl Chem 282(3):737–742. doi:10.1007/s10967-009-0207-3
10. Bowyer TW, Kephart R, Eslinger PW, Friese JI, Miley HS, Saey PRJ (2013) Maximum reasonable radioxenon releases from medical isotope production facilities and their effect on monitoring nuclear explosions. J Environ Radioact 115(1):192–200. doi:10.1016/j.jenvrad.2012.07.018
11. van Loef EVD, Dorenbos P, van Eijk CWE, Krämer K, Güdel HU (2000) High-energy-resolution scintillator: Ce^{3+} activated $LaCl_3$. Appl Phys Lett 77(10):1467–1468. doi:10.1063/1.1308053
12. Agostinelli S, Allison J, Amako K, Apostolakis J, Araujo H, Arce P, Asai M, Axen D, Banerjee S, Barrand G, Behner F, Bellagamba L, Boudreau J, Broglia L, Brunengo A, Burkhardt H, Chauvie S, Chuma J, Chytracek R, Cooperman G, Cosmo G, Degtyarenko P, Dell'Acqua A, Depaola G, Dietrich D, Enami R, Feliciello A, Ferguson C, Fesefeldt H, Folger G, Foppiano F, Forti A, Garelli S, Giani S, Giannitrapani R, Gibin D, Gómez Cadenas JJ, González I, Gracia Abril G, Greeniaus G, Greiner W, Grichine V, Grossheim A, Guatelli S, Gumplinger P, Hamatsu R, Hashimoto K, Hasui H, Heikkinen A, Howard A, Ivanchenko V, Johnson A, Jones FW, Kallenbach J, Kanaya N, Kawabata M, Kawabata Y, Kawaguti M, Kelner S, Kent P, Kimura A, Kodama T, Kokoulin R, Kossov M, Kurashige H, Lamanna E, Lampén T, Lara V, Lefebure V, Lei F, Liendl M, Lockman W, Longo F, Magni S, Maire M, Medernach E, Minamimoto K, Mora de Freitas P, Morita Y, Murakami K, Nagamatu M, Nartallo R, Nieminen P, Nishimura T, Ohtsubo K, Okamura M, O'Neale S, Oohata Y, Paech K, Perl J, Pfeiffer A, Pia MG, Ranjard F, Rybin A, Sadilov S, Di Salvo E, Santin G, Sasaki T, Savvas N, Sawada Y, Scherer S, Sei S, Sirotenko V, Smith D, Starkov N, Stoecker H, Sulkimo J, Takahata M, Tanaka S, Tcherniaev E, Safai Tehrani E, Tropeano M, Truscott P, Uno H, Urban L, Urban P, Verderi M, Walkden A, Wander W, Weber H, Wellisch JP, Wenaus T, Williams DC, Wright D, Yamada T, Yoshida H, Zschiesche D (2003) Geant4—a simulation toolkit. Nucl Instrum Methods A 506(3):250–303. doi:10.1016/S0168-9002(03)01368-8
13. NuDat (2014) NuDat 2.6 database, nuclear structure and decay data. National Nuclear Data Center, Brookhaven National Laboratory. http://www.nndc.bnl.gov/nudat2/. Accessed 20 Sept 2014
14. Eslinger PW, Cameron IM, Dumais JR, Imardjoko Y, Marsoem P, McIntyre JI, Miley HS, Stoehlker U, Widodo S, Woods VT (2015) Source term estimates of radioxenon released from the BaTek medical isotope production facility using external measured air concentrations. J Environ Radioact 148:10–15. doi:10.1016/j.jenvrad.2015.05.026